J Mol Model (2003) 9:9–15
DOI 10.1007/s00894-002-0103-z

ORIGINAL PAPER

Carlo Caporale · Angelo Facchiano · Laura Bertini · Luca Leonardi · Gabriele Chilosi · Vincenzo Buonocore · Carla Caruso

Comparing the modeled structures of PR-4 proteins from wheat

Received: 21 June 2002 / Accepted: 26 September 2002 / Published online: 7 February 2003

Abstract We have constructed three-dimensional models of four pathogenesis-related (PR) proteins from wheat (wheatwins) belonging to the PR-4 family. All the models were based on the knowledge of the tertiary structure of barwin, a highly homologous protein from barley. Wheatwin1 and wheatwin2 differ in two amino acid residues (positions 62 and 68) out of 125. Wheatwin4 differs from wheatwin2 in one residue at position 78, while wheatwin3 differs from wheatwin1 in one residue at position 88. The global folding and the secondary structures were very similar through all the sequences, including the regions of the amino acid substitutions. The main differences were found in the traits 15–21, 84–86 and 91–93. Trait 15–21 was predicted as ß-sheet in wheatwin4 and random-coil in the other proteins. Trait 84–86 was predicted as ß-sheet in wheatwin3 and random-coil in the other proteins. Trait 91–93 was predicted as random coil in wheatwin1 and wheatwin3 and ß-sheet in the other two proteins. Traits 15–21 and 84–86 were exposed, while trait 91–93 was quite hidden in all the proteins. The antifungal activities of the four proteins towards the specific pathogenic fungus *Fusarium culmorum* were distinct and well correlated to the structural differences. These results suggest that these regions may have a role in the action mechanism, which is still unknown.

C. Caporale (✉) · L. Bertini · L. Leonardi · V. Buonocore · C. Caruso
Dipartimento di Agrobiologia ed Agrochimica,
Università della Tuscia, Via S. Camillo de Lellis,
01100 Viterbo, Italy
e-mail: caporale@unitus.it
Fax: +39-0761-357242

A. Facchiano
Istituto di Scienze dell'Alimentazione – CNR, Via Roma 52 A/C,
83100 Avellino, Italy

G. Chilosi
Dipartimento di Protezione delle Piante, Universita' della Tuscia,
Viterbo, Italy

Keywords Protein structure · Surface accessibility · Pathogenesis related · Antifungal activity

Introduction

Plant–pathogen interaction produces many groups of pathogenesis-related (PR) proteins showing strong antifungal activity in vitro against pathogenic fungi. PR proteins were first detected in tobacco plants infected with tobacco mosaic virus: a large number of members of this protein family were later described in other plant species and grouped in 14 classes. [1] The antifungal properties of several PR proteins can be associated with their enzymatic or inhibitory activity (e.g. PR-2 are β-glucanases; PR-3, chitinases; PR-6, proteinase inhibitors; PR-9, peroxidases), whereas other proteins have still an unknown function. [1] In recent years, we have isolated and sequenced four PR-4 proteins from wheat kernels, named wheatwin1 to wheatwin4, that inhibit phytopathogenic fungi with a wide host range (e.g. *Botrytis cinerea*) and host-specific pathogens (e.g. *Fusarium culmorum*, *F. graminearum*). [2, 3, 4] We demonstrated that wheatwin1 and wheatwin2 are specifically induced in wheat seedlings infected with *Fusarium culmorum*; [5] their cDNAs have been cloned and the recombinant proteins expressed in *E. coli*. [6, 7] Also, the three-dimensional (3D) model of wheatwin1, based on the tertiary structure in solution of barwin, [8, 9] a highly homologous protein from barley [10] showing a six-stranded double-psi β barrel, [11] has been designed and experimentally validated. [12] Although wheatwin1 and wheatwin2 differ in just two amino acid residues, their antifungal activities are different, [3] suggesting that micro-differences in the 3D structures, probably due to side chain effects, influence the effectiveness of the protecting action. Proteins of the PR-4 family have been poorly described to date. Their action mechanism and their potential in enhancing plant resistance to pathogenic fungi and in amplifying the antifungal effects of other well-described PR proteins (osmotin, chitinase, glucanase) have not been explored at

all. With the aim of obtaining information on the action mechanism by identifying structurally distinct domains that could justify the different biological activity, we constructed 3D models of all the proteins. In fact, if spatial atom coordinates of a reference protein are provided, simulation procedures can be used to determine the 3D structure of homologous molecules. [13, 14, 15, 16 and references therein] The method is very useful and specific software dedicated to homology modeling (Swiss Model, Swiss PDB viewer, FAMS) is currently available on the World Wide Web. [17, 18, 19] As for the wheatwin1 model, [12] we used the NMR data of barwin [10] to build up the models of wheatwin2, wheatwin3 and wheatwin4. The models were compared and their structural differences discussed and related to the antifungal activity.

Materials and methods

Molecular modeling

Structure prediction of wheatwin proteins was based on the availability of the 3D model of the homologous protein barwin [8, 9, 10] (pdb code: 1bw3) and performed as described previously. [12] The alignment of wheatwin proteins and barwin did not require deletion or gap insertion. The programs MODELLER [20] and Quanta (Accelrys, Inc.) were used to build protein models according to the comparative protein modeling methodology. Similarly to our previous work, [12, 21] we created ten full-atom models for each protein by setting 4.0 Å as RMS deviation among initial models and full optimization of the models, i.e. multiple cycles of refining with conjugate gradients minimization and molecular dynamics with simulated annealing. Finally, the best model was selected on the basis of the Ramachandran plots evaluated with the program PROCHECK. [22] Secondary structures were assigned by the programs DSSP [23] and Swiss PDB Viewer. [17] The parameters used for the H-bond detection threshold were the following for all the models: minimum distance 1.200±0.05 Å, maximum distance 2.76±0.05 Å, minimum angle 120° when hydrogen was present; minimum distance 2.195±0.05 Å, maximum distance 3.30±0.05 Å, minimum angle 90° when hydrogen was not present. Search for structural classification of barwin was performed on the SCOP [24] and CATH [25] databases. Solvent accessibility of amino acids was evaluated by the program NACCESS, [26] calculating the atomic accessible surface defined by rolling a probe of 1.40 Å around the van der Waals surface of the protein models. Nicksite predictions were made by the online program NICKPRED (http://sjh.bi.umist.ac.uk/nickpred.html) [26, 27] using the default values of accessibility, protrusion index, flexibility, secondary structure, and main chain hydrogen bonding. Figures were drawn with Swiss PDB Viewer, [17] RasMol [28, 29] and the InsightII package (Accelrys, Inc.).

Antifungal activity

Wheatwin proteins were extensively dialyzed against distilled water and lyophilized. Inhibition bioassays of fungal growth were carried out using the wheat pathogenic fungus *Fusarium culmorum* (isolate ISPAVE485). Sporulating cultures were obtained by growing the isolate on Potato Dextrose Agar (PDA) (Oxoid – Unipath) at 24 °C for 14 days. Conidia were collected by scraping a sterile inoculating loop across the surface of the plate in the presence of 2x potato dextrose broth (PDB) (Sigma-Aldrich), and counted with a hemocytometer. In the growth inhibition assay, 5 µl aliquots of a suspension containing 10^4 ml^{-1} spores were placed on sterile microscope slides and 5 µl of protein solutions were added to each spore suspension (final protein concentration 5, 10, 25 and 50 µg ml^{-1}); the microscope slides were kept in a moist chamber at 21 °C in the dark for 15 h. Antifungal activity was determined microscopically by measuring hyphal growth; two sets of spore macroconidia suspension in sterile distilled water and in bovine serum albumin solution represented the controls. Assays were performed in duplicate and both the average of at least 100 measurements of hyphal growth for each sample and the standard deviations were calculated. The inhibition percentage of hyphal growth was calculated for each protein concentration. The effective doses for 50% inhibition (ED_{50}) were also calculated.

Results

Homology modeling

We recently constructed and validated the 3D model of wheatwin1 using the barwin 3D structure as reference. [12] Using the same procedure, we built up and refined the models of wheatwin2, wheatwin3 and wheatwin4. The stereochemical quality of models was assessed with the

Fig. 1 Homology alignment of the amino acid sequences of barwin and wheatwin proteins. Positions showing different residues are labeled by (-) and numbered. The top scoring seven nicksites are also indicated by italics. The colors indicate different secondary structures: *blue*=β-sheets; *red*=α-helices; *black*=coil

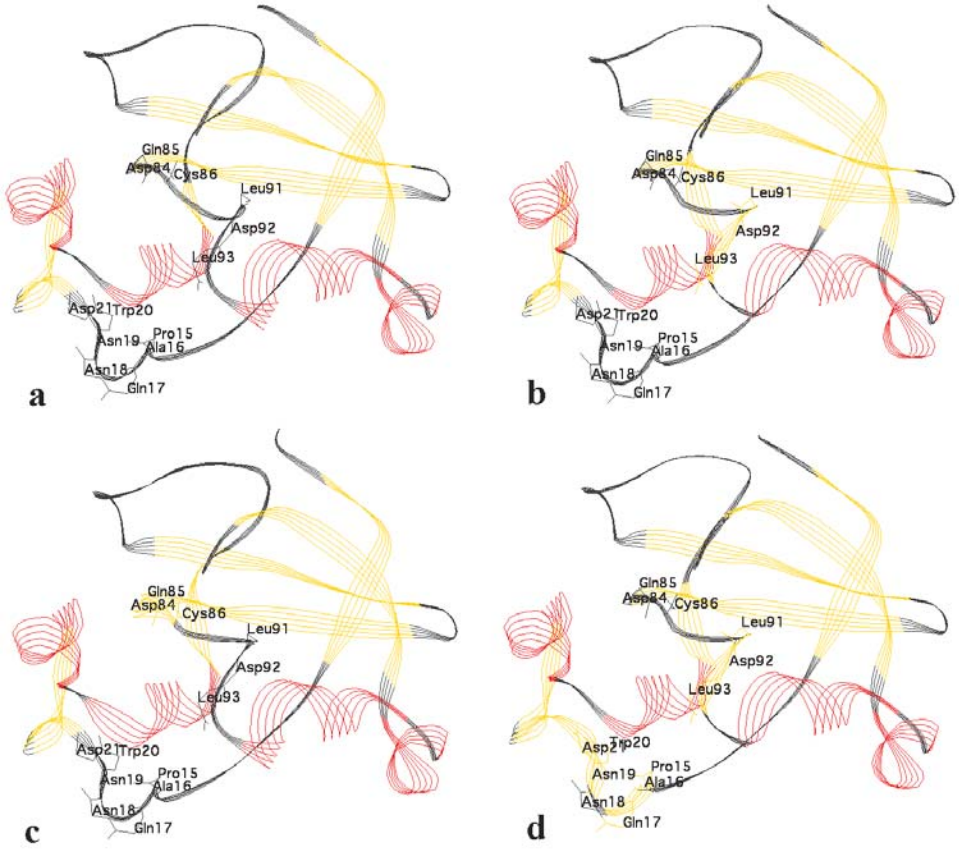

Fig. 2a–d Ribbon view of wheatwin1 (**a**), wheatwin2 (**b**), wheatwin3 (**c**) and wheatwin4 (**d**) models. The positions of the regions 15–21, 84–86 and 91–93 are labeled; secondary structures are marked by different colors: *yellow*=*β*-sheets; *red*=*α*-helices; *gray*=coil

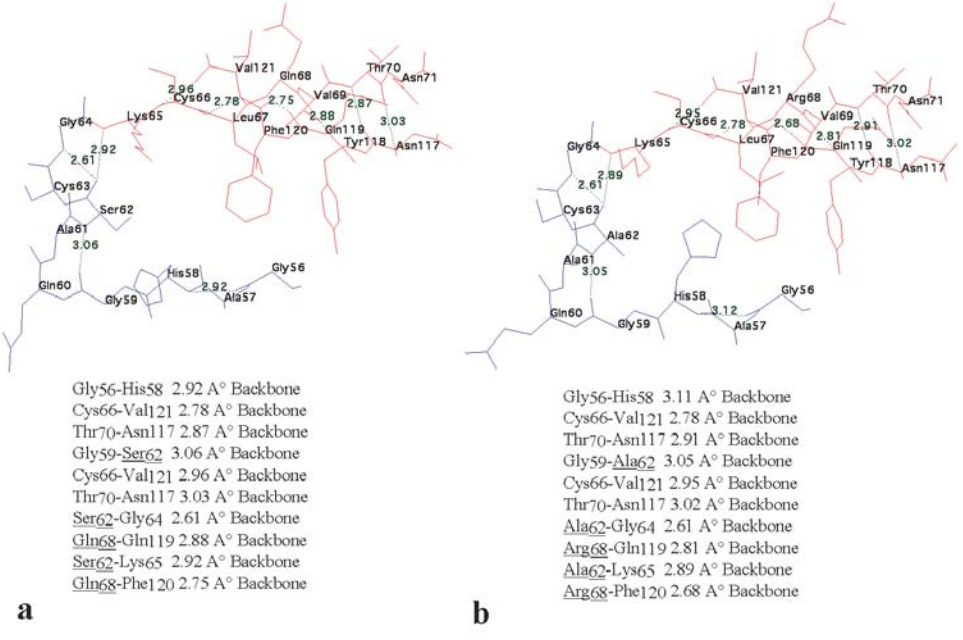

Fig. 3a,b H-bonds formed in the regions containing residues 62 and 68 of wheatwin1 (**a**) and wheatwin2 (**b**). The length and type of each bond are indicated

program PROCHECK. [22] The Ramachandran plots confirmed their excellence, the percentage of residues in most favored and additional allowed regions being no lower than 97.2 (not shown). The alignment of the sequences of wheatwin and barwin proteins, all possessing 125 residues, did not require deletion or gap insertion. The structural differences between all the wheatwins are localized at positions 62, 68, 78 and 88. Barwin shows four further substitutions localized at positions 4, 5, 57 and 58. It is identical in 118, 119, 120 and 121 residues

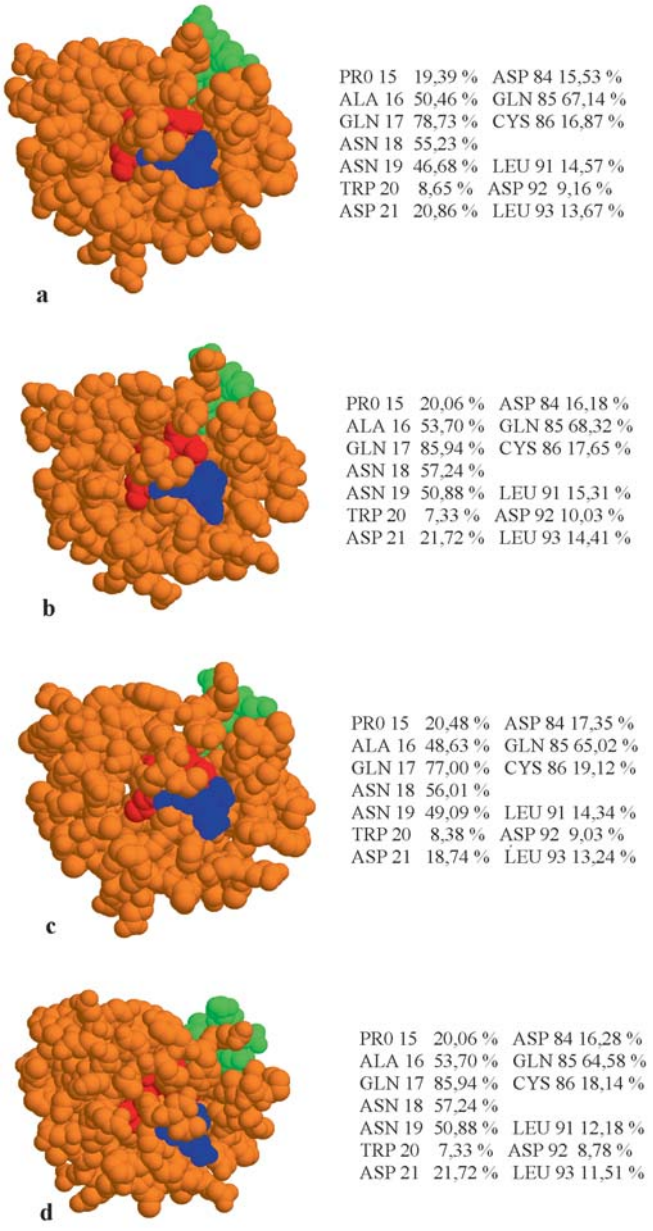

Fig. 4a–d Front side spacefill view of wheatwin1 (**a**), wheatwin3 (**b**), wheatwin2 (**c**) and wheatwin4 (**d**) models. The surface positions of regions 15–21 (*green*), 84–86 (*blue*) and 91–93 (*red*) are shown. The region 15–21 is protruding in all the molecules. The regions 84–86 and 91–93 are not visible on the back side. The solvent accessibility of each residue is indicated

out of 125 to wheatwin3, wheatwin1, wheatwin4 and wheatwin2, respectively (Fig. 1). As expected, the global folds of all the proteins were very similar, although some micro-differences in the secondary structures can be observed (Fig. 2). Different secondary structures are also emphasized by diverse color codes in Fig. 1. Wheatwin1 and wheatwin2 differ in two residues located at positions 62 and 68. These substitutions do not cause significant structural changes in the region. In fact, the secondary structures are identical (Fig. 1) since the regions 56–71 and 117–121 maintain an equal distance in the folding of both proteins although Ala 62 and Arg 68 in wheatwin2 replaced Ser 62 and Gln 68 in wheatwin1. As a consequence, the same ten backbone hydrogen bonds were formed (Fig. 3). Furthermore, the solvent accessibilities of the residues 62 and 68 are similar in both proteins. Residue 62 is quite hidden, while residue 68 is quite exposed (not shown). However, substitutions 62 and 68 induce changes in the secondary structure of the trait 91–93. This region shows the same solvent accessibility in both proteins (Fig. 4), but its distance from the region 48–50 is different in the two molecules. In fact, while the H-bonds Leu 91–Ala 50, Leu 93–Trp 48 (backbone) and Leu 91–Thr 49 and Thr 49–Ala 50 (side chain) were formed in wheatwin2, no bond was present in wheatwin1 (Fig. 5). As shown in Fig. 2, the region 91–93 of all the proteins is contained in a loop, but is predicted as coil in wheatwin1 (Fig. 2a) and wheatwin3 (Fig. 2c) while β-sheets characterize its structure in wheatwin2 (Fig. 2b) and wheatwin4 (Fig. 2d). The other differences in the amino acid sequences of wheatwins are at positions 78 and 88 (Fig. 1). As already observed for substitution 62 and 68, no change in the secondary structure was observed in the corresponding regions (Fig. 1) since the same H-bonds were formed (not shown). However, two further regions show different secondary structures in the four molecules. In particular, the trait 15–21 was predicted as ß-sheet in wheatwin4 and as coil in the other proteins, while the trait 84–86 was predicted as β-sheet in wheatwin3 and as coil in the other wheatwins (Figs. 1 and 2). The different H-bonds involved in the 15–21 region of wheatwin4 with respect to wheatwin2 (and the other two wheatwins) are shown in Fig. 6. Four backbone plus one side chain H-bonds were formed in wheatwin4, while three backbone plus one side chain H-bonds were present in the 15–21 region of wheatwin2. The extra H-bond present in wheatwin4, as well as the different disposition of the others, causes the change in the secondary structures. Finally, the trait 84–86 was similarly exposed in all the proteins (Fig. 4), but three H-bonds were formed in wheatwin3, while just one was present in wheatwin1 and the other proteins (Fig. 7), justifying the different secondary structures.

NICKPRED prediction

The micro-differences in the wheatwin structures were further investigated by using the on-line program NICKPRED. [26, 27] This software, working with spatial atom coordinates contained in PDB data files, is well suited to predicting protein surface features other than proteolytic susceptibility. In fact, the algorithm uses a set of conformational parameters such as accessibility, protrusion index, flexibility, secondary structure, main chain hydrogen bonding and low local mobility of cysteines involved in disulphide bridges. Proteolytic sites are usually accessible, protruding and flexible, the most common being coiled (loops, turns, etc); sheet nicksites

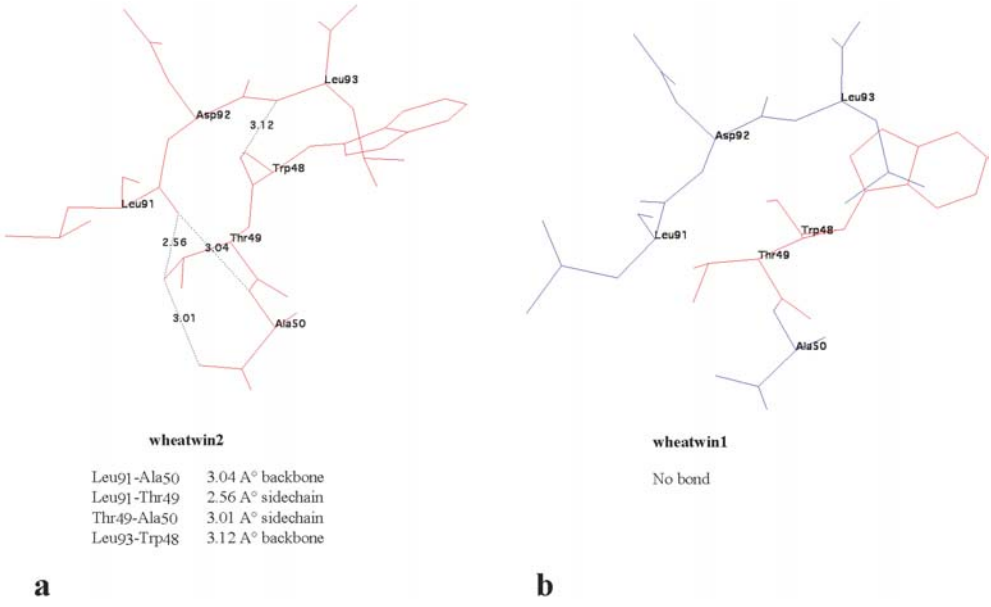

Fig. 5a,b H-bonds formed in the regions 91–93 of wheatwin2 (**a**) and wheatwin1 (**b**). The length and type of each bond are indicated. No bond was formed in wheatwin1

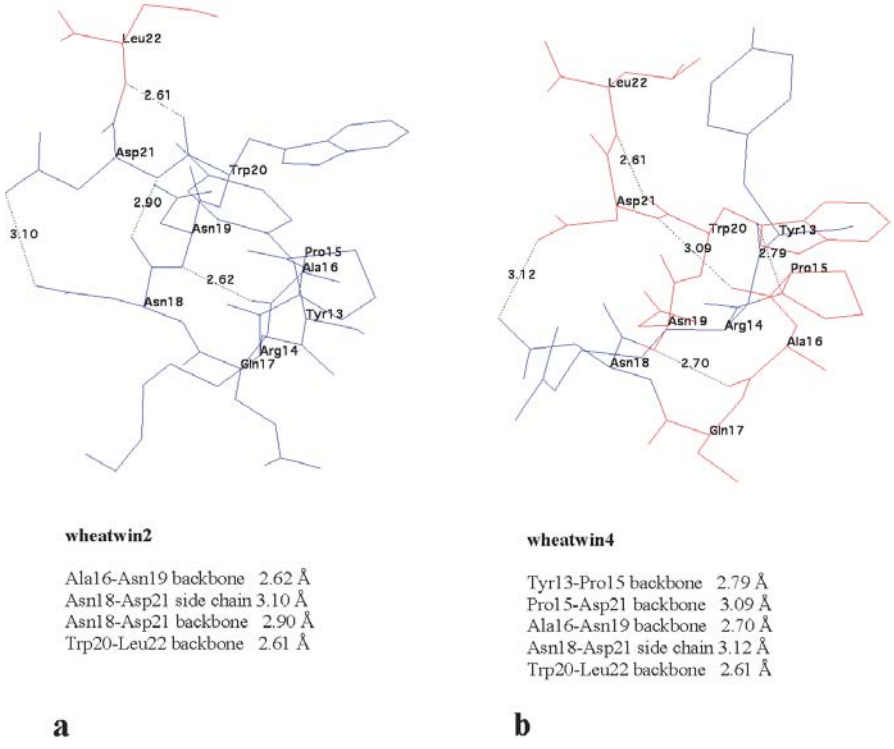

Fig. 6 H-bonds formed in the regions 15–21 of wheatwin2 (**a**) and wheatwin4 (**b**). The length and type of each bond are indicated

are extremely rare, while helices are less disfavored. [27] The results obtained using aspecific (general) proteases and default parameters of the program for nicksite prediction of the four wheatwins are shown in Fig. 1. The top scoring seven sites for each protein are indicated with 1–7. Four sites of wheatwin1 and wheatwin3 are localized at positions 19, 20, 21 and 22, while the same regions of wheatwin2 and wheatwin4 contain two and one, respectively. No top-scoring nicksite was contained in the regions 84–86 and 91–93.

Antifungal activity

The antifungal activities of wheatwins against the wheat pathogen *Fusarium culmorum* were determined by measuring the inhibition of hyphal growth at various protein concentrations (5–50 μg ml^{-1}). The results obtained using a final protein concentration of 25 μg ml^{-1} are summarized in Table 1. Wheatwin1 and wheatwin3 were the most effective. Wheatwin2 exhibited minor activity, while wheatwin4 was the least effective. Similar results

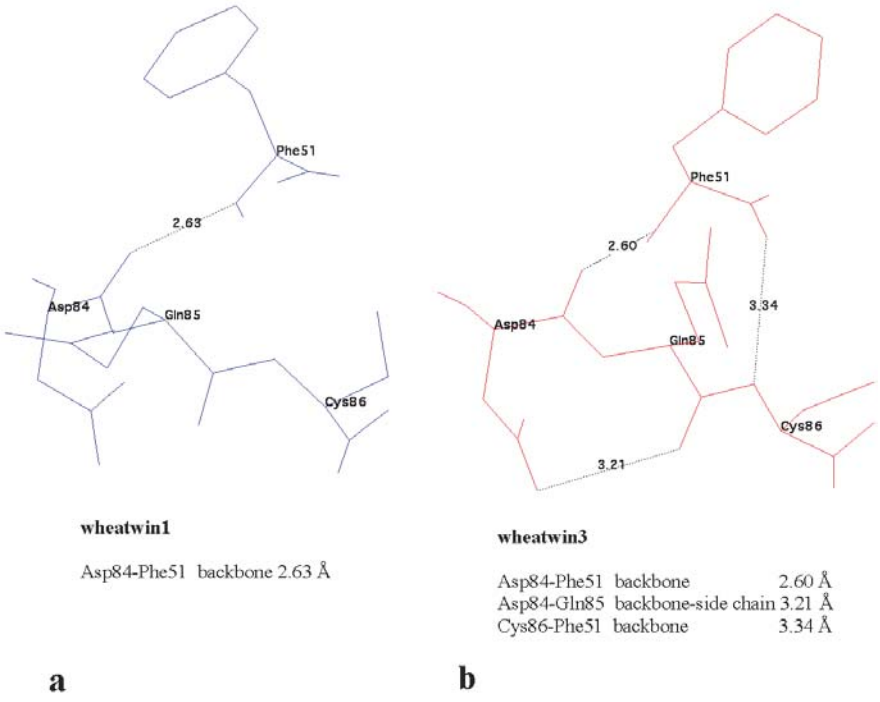

Fig. 7 H-bonds formed in the regions 84–86 of wheatwin1 (**a**) and wheatwin3 (**b**). The length and type of each bond are indicated

Table 1 Antifungal activity of wheatwin proteins against *F. culmorum*. Regions with different secondary structures are indicated

Protein	Hyphal growth inhibition (%)	Region 91–93	Region 15–21	Region 84–86
Wheatwin1	37.6±0.8	Coil	Coil	Coil
Wheatwin3	36.3±1.2	Coil	Coil	β-Sheet
Wheatwin2	27.4±1.3	β-Sheet	Coil	Coil
Wheatwin4	15.4±0.9	β-Sheet	β-Sheet	Coil

were obtained at the other protein concentrations (not shown).

Discussion

The use of an NMR-derived structure as the template protein may lead to the conclusion that significant backbone differences found between very similar proteins could be modeling artifacts rather than being genuine. In fact, the side chains are likely to be less well resolved than an X-ray, and errors in initial side chain placement might alter the results of the refinement. However, this should not be the case for the wheatwin proteins. In fact, an identical procedure was carried out to build up and refine the four models. On the other hand, the diverse antifungal activities can only be due to micro-differences in the global folding of the four molecules. The micro-differences predicted in the secondary structures of regions 91–93, 15–21 and 84–86 correlate well with the biological activities. The region 91–93, showing a coil structure in wheatwin1 and wheatwin3, should be more flexible in these two proteins and, if involved in the action mechanism, should have a better interaction with the pathogen molecular target, allowing these two proteins to exert a stronger antifungal activity. In fact, the local flexibility is high in coil regions, minor in helices and low in β-sheets. [26, 27] For the same reason, the region 15–21 should be less flexible in wheatwin4 than in the other proteins. If involved in the defense mechanism, it should have a major role since it is very accessible and protruding in all the proteins (Fig. 4) and, like 91–93, is located in a loop (Fig. 2). However, it should be stressed that these considerations are based on data models derived from a static analysis. We are planning to perform a dynamic analysis by MD simulations to confirm and reinforce these conclusions.

The results obtained by nicksite prediction confirmed that the region 15–21 has a good solvent accessibility in all the proteins, but only minor mobility in wheatwin4 since just one top-scoring site was identified. No further NICKPRED information was gained for residues in the regions 84–86 and 91–93, probably due to the presence of Cys 86, which is involved in a disulphide bridge.

The differences in the secondary structures could be correlated to the diverse antifungal effectiveness of the four wheatwins (Table 1). Wheatwin1 and wheatwin3 were the most effective, both possessing coil structures in the regions 91–93 and 15–21. Wheatwin2 showed minor activity, the region 91–93 being predicted to be ß-sheet,

while wheatwin4 was the least potent, with both regions predicted to be ß-sheet. The structure of the region 84–86 does not seem to influence differentiating the antifungal activity. The antifungal activity of the reference protein barwin, whose structure has been fully determined, [8, 9, 10] has not been described. The only report on the antifungal activity of PR-4 proteins from barley regards three isoproteins, closely related to barwin, whose amino acid sequences have been partially assessed. [30] However, a direct comparison of the antifungal activity of these proteins and wheatwins cannot be done, since the determination methods and the pathogen fungi used are different. Microscopic examination indicated that the activity of wheatwins is directed toward the fungal membrane, presumably by affecting permeability of cytoplasmic material (Chilosi et al. 2002, submitted for publication). A similar effect has been reported for thaumatin-like proteins belonging to the PR-5 family. [31 and references therein] Like PR-4, PR-5 proteins cause inhibition of hyphal growth and reduction of spore germination. [31] The crystal structures of thaumatin and its homologous protein zeamatin have also been determined. [32, 33] The zeamatin surface is electrostatically polarized. The cleft on the front side is acidic, whereas the back side is predominantly basic. It has been proposed that the acidic cleft may interact electrostatically with some molecule in the fungal cell (e.g. a channel or receptor protein) resulting in an influx of water or ion. [31] Anyway, the structures of PR-4 and PR-5 proteins are completely unrelated. In fact, zeamatin possesses 206 amino acid residues and 16 cysteines all involved in disulphide bridges to stabilize the protein structure. It has 13 β-strands, 11 of which form a β-sandwich representing the core of the protein. [33] Furthermore, the charge distribution of wheatwins is totally different (not shown). So, it can be supposed that, although the macroscopic effects of the antifungal activity of PR-4 and PR-5 proteins are similar, the action mechanism and/or the fungal molecular target are distinct.

Conclusions

The micro-differences in the structure of four wheatwin proteins have been assessed by comparative homology modeling to correlate their structure–function relationships. The regions 15–21 and 91–93 should be important in the interaction with the pathogen molecular target since they have similar solvent accessibilities but different secondary structures, and such differences are correlated to their diverse antifungal activities. These results should contribute to the assessment of PR-4 proteins' action mechanism, which is still unknown.

Acknowledgements This research was supported by a grant from Consorzio Interuniversitario Biotecnologie (CIB).

References

1. Van Loon LC, Van Strien EA (1999) Physiol Mol Plant Pathol 55:85–97
2. Caruso C, Caporale C, Poerio E, Facchiano A, Buonocore V (1993) J Protein Chem 12:379–386
3. Caruso C, Caporale C, Chilosi G, Vacca F, Bertini L, Magro P, Poerio E, Buonocore V (1996) J Protein Chem 15:35–44
4. Caruso C, Nobile M, Leonardi L, Bertini L, Buonocore V, Caporale C (2001) J Protein Chem 20:327–335
5. Caruso C, Chilosi G, Caporale C, Bertini L, Magro P, Buonocore V (1999) Plant Sci 140:87–97
6. Caruso C, Bertini L, Tucci M, Caporale C, Leonardi L, Saccardo F, Bressan R, Veronese P, Buonocore V (1999) DNA Sequence 10:301–307
7. Caruso C, Bertini L, Tucci M, Caporale, Nobile M, Leonardi L, Buonocore V (2001) Protein Expr Purif 23:380–388
8. Ludvigsen S, Poulsen FM (1992) Biochemistry 31:8771–8782
9. Ludvigsen S, Poulsen FM (1992) Biochemistry 31:8783–8789
10. Svensson B, Svendsen I, Hojrup P, Roepstorff P, Ludvigsen S, Poulsen FM (1992) Biochemistry 31:8767–8770
11. Castillo RM, Mizuguchi K, Dhanaraj V, Albert A, Blundell TL, Murzin AG (1999) Structure Fold Des 15:227–236
12. Caporale C, Caruso C, Facchiano A, Nobile M, Leonardi L, Bertini L, Colonna G, Buonocore V (1999) Proteins 36:192–204
13. Lesk AM, Tramontano A (1992) Binary 4:15–16
14. Lesk A, Tramontano A (1989) J Res Natl Inst Stand Technol 94:85–93
15. Chothia C, Lesk AM (1986) EMBO J 5:823–826
16. Blundell TL, Sibanda LB, Sternberg MJ, Thornton JM (1987) Nature 326:347–352
17. Guex N, Peitsch MC (1997) Electrophoresis 18:2714–2723
18. Guex N, Diemand A, Peitsch MC (1999) TIBS 24:364–367
19. Ogata K, Umeyama H (2000) J Mol Graph Model 18:258–272
20. Sali A, Blundell TL (1993) J Mol Biol 234:779–815
21. Facchiano AM, Stiuso P, Chiusano ML, Caraglia M, Giuberti G, Marra M, Abbruzzese A, Colonna G (2001) Protein Eng 14:881–890
22. Laskowski RA, MacArthur MW, Moss DS, Thornton JM (1993) J Appl Crystallogr 26:283–291
23. Kabsch W, Sander C (1983) Biopolymers 22:2577–2637
24. Murzin AG, Brenner SE, Hubbard T, Chothia C (1995) J Mol Biol 247:536–540
25. Orengo CA, Michie AD, Jones S, Jones DT, Swindells MB, Thornton JM (1997) Structure 5:1093–1108
26. Hubbard SJ, Campbell SF, Thornton JM (1990) J Mol Biol 220:507–530
27. Hubbard SJ, Eisenmenger F, Thornton JM (1994) Protein Sci 3:757–768
28. Sayle RA, Milner-White EJ (1995) Trends Biochem Sci 20:374–376
29. Bernstein HJ (2000) Trends Biochem Sci 25:453–455
30. Hejgaard J, Jacobsen S, Bjørn SE, Kragh KM (1992) FEBS Lett 307:389–392
31. Kitajjima S, Sato F (1999) J Biochem 125:1–8
32. Ogata CM, Gordon PF, Kim SH (1992) J Mol Biol 228:893–908
33. Batalia MA, Monzingo AF, Ernst S, Roberts W, Robertus JD (1996) Nat Struct Biol 3:19–23